Efficient and versatile aberration correction through sensorless adaptive optics

Qi Hu[a], Martin Hailstone[a], and Martin Booth[a]

[a]University of Oxford, Oxford, UK

ABSTRACT

Wavefront-sensorless adaptive optics methods are often used to correct phase aberrations in optical systems and thus to improve imaging quality. However, sensorless methods have an intrinsic disadvantage of requiring multiple images that can lead to non-desirable photo-bleaching. We have proposed a machine learning assisted aberration correction method which could correct aberrations consisting of not fewer than five Zernike modes with as few as two images. We showed that our method could be used in microscopes to provide instant aberration predictions when imaging biological samples of non-specific structures. We showed that compared to conventional function fitting sensorless adaptive optics methods, the new method corrected much faster with observable advantages. This novel method has a great potential to be used in any adaptive optics equipped microscopy for efficient sensorless aberration correction for biomedical microscopy.

Keywords: Aberrations, adaptive optics, microscopy

1. INTRODUCTION

The imaging quality of microscopes is limited by phase aberrations due to optical inhomogeneities in specimens and inherent limitations of optical systems. Adaptive optics (AO) can actively modulate the phase of wavefronts and is thus often used to compensate aberrations and restore near-diffraction-limited operation.[1–5] Phase aberration correction is achieved by estimating aberrations through the use of a wavefront sensor or through indirect optimisation approaches. Although direct wavefront sensing methods are often used for their fast processing speed, wavefront-sensorless aberration correction methods (known concisely as "sensorless AO") are favoured in many cases for their compact and simple optical designs. Furthermore, sensorless approaches do not suffer from non-common-path sensing errors. There are also cases where the signal level is too low for sensor-based methods to be feasible, leaving sensorless methods the only viable option.

One disadvantage of sensorless AO methods is that they normally require multiple images over the same field of view to gather enough information for effective phase retrieval. Prolonged sample exposures can lead to photobleaching, which is not desirable, or cause problems due to specimen motion. Some work in the literature has investigated the design of machine learning assisted efficient sensorless AO methods to correct phase aberrations with fewer sample exposures. However, they either are limited to work on point spread functions (PSFs) obtained from images of point like objects[6–10] or require several minutes of processing time.[11,12] These methods are thus not ideal for use during live biological imaging, where PSFs may not always be obtainable for the chosen optical system, point-like objects may not always exist in the chosen biological sample and the processing speed is critical.

In this paper, we present an efficient machine learning based aberration correction method that can work on different AO equipped microscopy modalities with no specific requirement on optical design. The method can correct aberrations when imaging complex and extended biological samples with a minimum of two images. The method used a pre-trained neural network and thus the processing time was negligible comparing to the time needed for the image acquisition or adapting the AO correction element.

Three-Dimensional and Multidimensional Microscopy: Image Acquisition and Processing XXIX, edited by Thomas G. Brown, Tony Wilson, Laura Waller, Proc. of SPIE Vol. 11966, 1196605 · © 2022 SPIE · 1605-7422 · doi: 10.1117/12.2610971

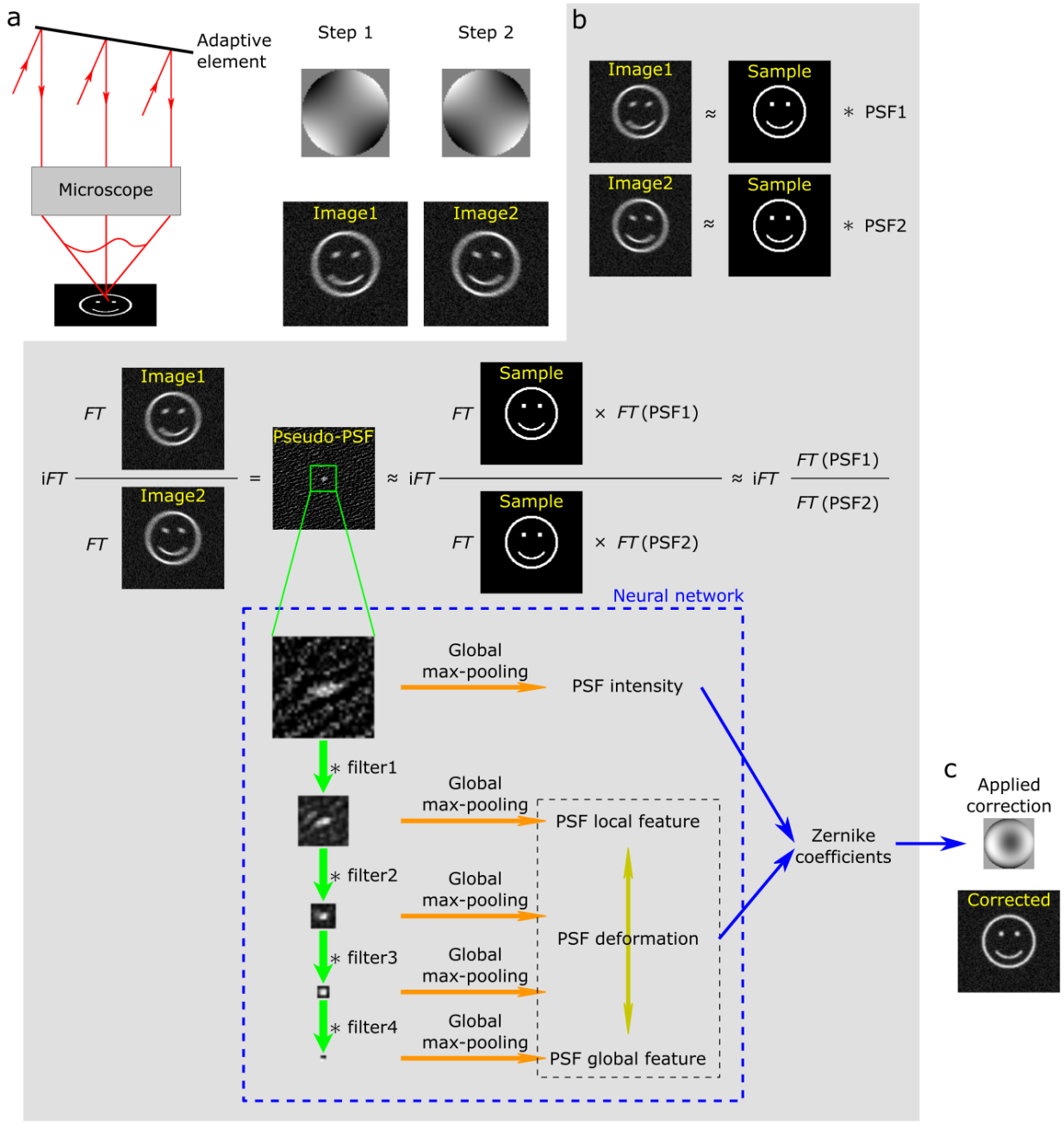

Figure 1. A schematic plot of the aberration correction process and working principle of the proposed machine learning based method. a: shows that our method requires at least two microscope images over the same field of view; each image is captured when a different phase modulation is applied with the adaptive element. In this case, we chose +1 rad and -1 rad of oblique astigmatism as our phase modulations. b: shows the basic working principle of our method. Images can be expressed mathematically as a convolution between the sample structure and PSFs. Therefore, by calculating the ratio between the Fourier transformed image1 and the Fourier transformed image2, we obtained a so-called"pseudo-PSF", which in theory contains only PSF related information. *FT* represents Fourier transform. Pseudo-PSFs are the inputs to a trained convolutional neural network, which can extract information related to both the PSF intensity and PSF deformations which are then used to deduce Zernike coefficients representing the aberration in the system. c: shows that the predicted Zernike coefficients are applied by the AO to acquire an aberration corrected image.

How do I apply phase modulations in FPM system? I don't have an adaptive element…

2. METHOD

The microscope image generation process can in many cases be modelled a convolution between sample structure and a PSF (Figure 1).

$$\text{Image}_1 \approx \text{sample} * \text{PSF}_1$$
$$\text{Image}_2 \approx \text{sample} * \text{PSF}_2$$

where $*$ represents the convolution operation. As aberration effects are contained entirely within the PSF, we would like to extract PSF-only information and to remove sample structures. So, we can divide the Fourier transforms of two images taken over the same field of view (FOV) but with different applied aberrations. Mathematically, this can be written as

$$\begin{aligned}\mathcal{FT}^{-1}\left[\frac{\mathcal{FT}(\text{Image}_1)}{\mathcal{FT}(\text{Image}_2)}\right] &\approx \mathcal{FT}^{-1}\left[\frac{\mathcal{FT}(\text{sample} * \text{PSF}_1)}{\mathcal{FT}(\text{sample} * \text{PSF}_2)}\right] \\ &\approx \mathcal{FT}^{-1}\left[\frac{\mathcal{FT}(\text{sample}) \times \mathcal{FT}(\text{PSF}_1)}{\mathcal{FT}(\text{sample}) \times \mathcal{FT}(\text{PSF}_2)}\right]\end{aligned}$$

Therefore, we can derive a function that we call the"pseudo-PSF", as it is defined in the same space as the PSF, although derived indirectly from the two images:

$$\mathcal{FT}^{-1}\left[\frac{\mathcal{FT}(\text{Image}_1)}{\mathcal{FT}(\text{Image}_2)}\right] \approx \mathcal{FT}^{-1}\left[\frac{\mathcal{FT}(\text{PSF}_1)}{\mathcal{FT}(\text{PSF}_2)}\right] = \text{pseudo-PSF}$$

By processing images to generate pseudo-PSFs, effects of sample structures are mostly removed. For these reasons, pseudo-PSFs are chosen as the input for the latter phase retrieval computations and aberration correction processes. Some residual effects of the sample structure may still be present, for example if the sample spectrum contains zero or near-zero values. However, these effects are not problematic, due to later processing steps.

A similar form of pre-computation was also used in[13] to post process images using a long short-term memory (LSTM) network with a stack of in-focus and out-of-focus images as the input. We calculated pseudo-PSFs to determine phase aberrations using a novel convolutional neural network (CNN) architecture specifically designed for our application; we then integrated phase aberration correction methods into AO microscopes to improve the imaging quality. We acquired input images with bias aberration modes intentionally introduced using the AO. this design had observable advantages over using a three dimensional image stack, especially in realistic microscope applications. This is because the three dimensional structures of biological samples mean that sample structures can change significantly between defocussed planes thus removing the advantages of the computation outlined above. In this paper, we demonstrated specifically the use of astigmatism as the chosen bias mode, although other choices of bias mode are possible.

3. RESULTS

We compared the novel trained CNN based method against two conventional parabolic fitting algorithms (known as 2N+1[14] and 3N[15]) to correct the same aberrations when imaging samples on a two-photon (2-P) microscope equipped with a spatial light modulator (SLM) as the adaptive correction element. The bias amplitude for phase modulation used in all three methods was chosen as 1 radian to enable a fair comparison. The corrections of the three algorithms were compared and presented in Figure 2.

Figure 2 a and b showed correction results when imaging $2\mu m$ beads clusters. The three methods are used to correct aberrations consist of five Zernike modes (oblique and vertical astigmatism, vertical and horizonal coma and spherical). Figure 2 c showed correction results when imaging microtubules of BPAE cells. The methods are used to correct aberrations consist of nine Zernike modes (oblique and vertical astigmatism, vertical and horizonal coma, vertical and oblique trefoil, spherical, oblique and vertical secondary astigmatism). For our

Further author information: (Send correspondence to Martin J. Booth)
Martin J. Booth: E-mail: martin.booth@eng.ox.ac.uk

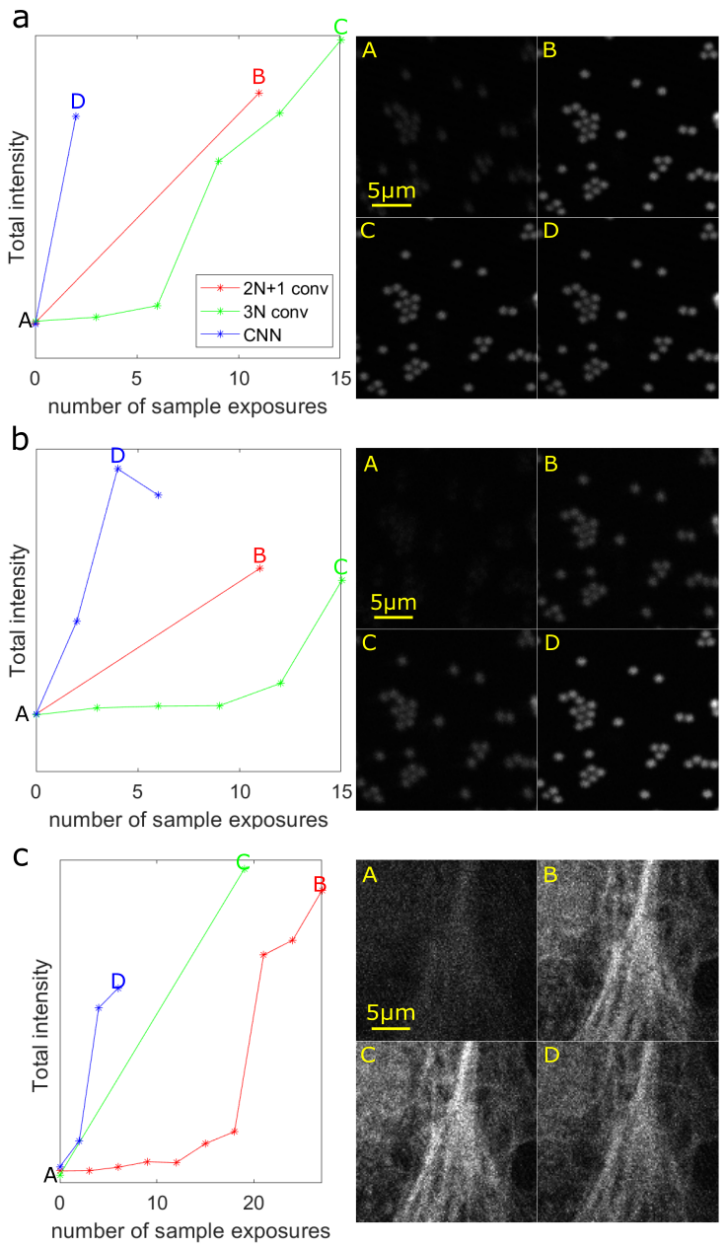

Figure 2. a, b and c showed three sets of results collected on a SLM equipped 2-P microscope when correcting the same aberrations using the three algorithms (2N+1 parabolic fitting, 3N parabolic fitting and our CNN based method). The plots showed the total fluorescence intensity varies with the number images captured for aberration correction processes. As indicated in the legend, the red coloured plots showed results using 2N+1 parabolic fitting algorithm; the green coloured plots showed results using 3N parabolic fitting algorithm; the blue coloured plots showed results using our CNN based algorithm. a and b were collected when imaging $2\mu m$ beads clusters for five Zernike modes. c was collected when imaging microtubules of bovine pulmonary artery endothelial (BPAE) cells and nine Zernike modes instead of five were corrected. The images used in c were significantly dimmer than those in a and b to demonstrate a case with low signal to noise ratio (SNR). The insets show single-frame raw images that correspond to the letters marked on the total intensity plot.

CNN based method, two images were required for each iteration correcting five Zernike modes (Figure 2 a and b) or nine Zernike modes (Figure 2 c). Note that the same trained CNN was used to generate the results in Figure 2 a and b. The trained CNN used to generate the results in Figure 2 c was a different network with a very similar architecture to that used in a and b. The only difference in the network architecture was that the output Zernike coefficients are changed from a size of five (Figure 2 a and b) to a size of nine (Figure 2 c). The two networks were separately trained using the same methodology. For 2N+1 method, 11 images were required to correct five modes (Figure 2 a and b) or 19 images are required to correct nine modes (Figure 2 c). For the 3N method, three images were required to correct each mode; therefore a total of 15 images were required to correct all five modes (Figure 2 a and b) or 27 images were required to correct nine modes (Figure 2 c).

The results suggested that among the three methods, the CNN based algorithm corrected aberrations the fastest in general (that is in terms of the rate of correction per image acquired) and could work on samples containing different structures. For dim samples, the CNN performed less advantageously but still corrected faster initially than the two conventional algorithms (see Figure 2 c for the plot gradients). This was what we would expect since CNN used only two images as its input and thus aberration prediction relied mainly on changes in the PSF shape. With a high noise level, the fine details changing in the PSFs are less observable. Since only two images were taken in each cycle, the CNN might also misinterpret noise as PSF related information and provide erroneous aberration predictions.

Furthermore, Figure 2 a, b and c showed that with just two images, the CNN method was not limited to correct only a specific number of modes. This showed that the method should be generalisable and could be adapted for different requirements using the same methodology.

4. CONCLUSIONS

We demonstrated a CNN based aberration correction method that can correct aberrations consisting of not fewer than five Zernike modes with as few as two images when imaging samples of different structures and brightness. The comparisons showed that in general our method corrected faster than conventional parabolic fitting algorithms. We showed that our method should not be limited to a certain choice of modes and could be adapted for different requirements as desired. The overall principle of this method is not limited to a particular microscope modality or optical design and could be adapted for a wide range of applications.

One potential downside is that this CNN based method could be more sensitive to noise than conventional algorithms since it depended on PSF deformations and such information could be less observable in noisy situations. CNN based method with more than two input images may allow the algorithm to be more robust against noise. The performance of such algorithms will be investigated in our later publications.

ACKNOWLEDGMENTS

This work was supported by European Research Council Award Grant No. AdOMiS 695140.

REFERENCES

[1] Booth, M. J., "Adaptive optics in microscopy," *Philosophical Transactions of the Royal Society of London A: Mathematical, Physical and Engineering Sciences* **365**(1861), 2829–2843 (2007).

[2] Booth, M. J., "Adaptive optical microscopy: the ongoing quest for a perfect image," *Light: Science & Applications* **3**(4), e165–e165 (2014).

[3] Booth, M. J. and Patton, B. R., "Adaptive Optics for Fluorescence Microscopy," in [*Fluorescence Microscopy: Super-Resolution and other Novel Techniques*], Cornea, A. and Conn, P. M., eds., 15–33, Academic Press, Boston (2014).

[4] Booth, M., Andrade, D., Burke, D., Patton, B., and Zurauskas, M., "Aberrations and adaptive optics in super-resolution microscopy," *Microscopy* **64**, 251–261 (06 2015).

[5] Ji, N., "Adaptive optical fluorescence microscopy," *Nature Methods* **14**(4), 374–380 (2017).

[6] Jin, Y., Zhang, Y., Hu, L., Huang, H., Xu, Q., Zhu, X., Huang, L., Zheng, Y., Shen, H.-L., Gong, W., and Si, K., "Machine learning guided rapid focusing with sensor-less aberration corrections," *Opt. Express* **26**, 30162–30171 (Nov 2018).

[7] Möckl, L., Petrov, P. N., and Moerner, W. E., "Accurate phase retrieval of complex 3D point spread functions with deep residual neural networks," *Applied Physics Letters* **115**(25), 251106 (2019).

[8] Vishniakou, I. and Seelig, J. D., "Wavefront correction for adaptive optics with reflected light and deep neural networks," *Opt. Express* **28**, 15459–15471 (May 2020).

[9] Saha, D., Schmidt, U., Zhang, Q., Barbotin, A., Hu, Q., Ji, N., Booth, M. J., Weigert, M., and Myers, E. W., "Practical sensorless aberration estimation for 3D microscopy with deep learning," *Opt. Express* **28**, 29044–29053 (Sep 2020).

[10] Cumming, B. P. and Gu, M., "Direct determination of aberration functions in microscopy by an artificial neural network," *Opt. Express* **28**, 14511–14521 (May 2020).

[11] Wang, F., Bian, Y., Wang, H., Lyu, M., Pedrini, G., Osten, W., Barbastathis, G., and Situ, G., "Phase imaging with an untrained neural network," *Light: Science & Applications* **9**(1), 77 (2020).

[12] Bostan, E., Heckel, R., Chen, M., Kellman, M., and Waller, L., "Deep phase decoder: self-calibrating phase microscopy with an untrained deep neural network," *Optica* **7**, 559–562 (Jun 2020).

[13] Xin, Q., Ju, G., Zhang, C., and Xu, S., "Object-independent image-based wavefront sensing approach using phase diversity images and deep learning," *Opt. Express* **27**, 26102–26119 (Sep 2019).

[14] Débarre, D., Booth, M. J., and Wilson, T., "Image based adaptive optics through optimisation of low spatial frequencies," *Opt. Express* **15**, 8176–8190 (Jun 2007).

[15] Facomprez, A., Beaurepaire, E., and Débarre, D., "Accuracy of correction in modal sensorless adaptive optics," *Optics Express* **20**, 2598 (Jan 2012).